Published in final edited form as:
Biochim Biophys Acta. 2009 May ; 1789(5): 413–421. doi:10.1016/j.bbagrm.2009.03.005.

The Chromatin Targeting Protein Brd2 is Required for Neural Tube Closure and Embryogenesis

Aron Gyuris[1], **Diana J. Donovan**[1], **Kimberly A. Seymour**, **Lindsay A. Lovasco**, **Nathaniel R. Smilowitz**, **Anthony L. P. Halperin**, **Jan E. Klysik**, and **Richard N. Freiman**[*]
Department of Molecular and Cell Biology and Biochemistry, Brown University, Providence, Rhode Island, 02903, USA

Abstract

Chromatin modifications are essential for directing transcription during embryonic development. Bromodomain-containing protein 2 (Brd2; also called RING3 and Fsrg1) is one of four BET (bromodomain and extra terminal domain) family members known to selectively bind acetylated histones H3 and H4. Brd2 associates with multiple subunits of the transcriptional apparatus including the mediator, TFIID and Swi/Snf multi-protein complexes. While molecular interactions of Brd2 are known, the functions of Brd2 in mammalian embryogenesis remain unknown. In developing a mouse model deficient in Brd2, we find that Brd2 is required for the completion of embryogenesis and proper neural tube closure during development. Embryos lacking *Brd2* expression survive up to embryonic day 13.5, soon after mid-gestation, and display fully penetrant neurulation defects that largely result in exencephaly of the developing hindbrain. In this study, we find that highest expression of *Brd2* is detected in the developing neural tube, correlating with the neural tube defects found in Brd2-null embryos. Additionally, embryos lacking *Brd2* expression display altered gene expression programs, including the mis-expression of multiple genes known to guide neuronal development. Together these results implicate essential roles for Brd2 as a critical integrator of chromatin structure and transcription during mammalian embryogenesis and neurogenesis.

Keywords

Chromatin; Transcription; Brd2; Neurogenesis; Neural Tube Closure; Spina Bifida

Introduction

Bromodomains are conserved chromatin-targeting modules found in many eukaryotic transcriptional regulatory proteins and have been shown to bind specifically to acetylated histones H3 and H4 [1–5]. Brd2 belongs to the BET subfamily of bromodomain proteins that contain two tandem N-terminal bromodomains (B) and a single C-terminal extra-terminal (ET) domain [6]. Epigenetic modifications of chromatin structure, such as histone acetylation and methylation, are known to have important consequences in the regulation of gene transcription [7]. Therefore, understanding the roles of murine Brd2 in interpreting combinatorial histone

*Correspondence to Richard N. Freiman, Department of Molecular and Cell Biology and Biochemistry, Brown University, 70 Ship St., Box G-E4, Providence, RI 02903, Phone: (401) 863-9633, FAX: (401) 863-9653: EMAIL: Richard_Freiman@Brown.edu.
[1]These authors contributed equally to this work.

modification of chromatin is a critical part of investigating the regulation of transcription during mammalian development.

Brd2 structure is conserved among plants, animals and fungi [6]. The yeast orthologs of Brd2, TFIID-associated components bromodomain factors 1 and 2 (Bdf1 and Bdf2), have been shown to be required for anti-silencing functions at subtelomeric regions of the yeast genome and for correctly interpreting histone modifications [2,8,9]. In Drosophila, Brd2 is most closely related to female sterile homeotic 1 (fsh1), a trithorax-group gene required for proper gene expression and fly embryogenesis [10–12]. Three of the four mammalian BET proteins—Brd2, Brd3 and Brd4—are broadly expressed, while the fourth, Brdt, is selectively expressed in the germline [13,14]. In the mouse, the ubiquitously expressed Brd2 has the highest levels of expression during embryogenesis as well as in the adult testis, ovary and brain [13–16]. Brd2 was initially identified as a nuclear kinase in human cells that is involved in guiding the expression of cell cycle genes through its binding to multiple E2Fs [17–19]. In addition, Brd2 has been shown to be associated with several multiprotein regulators of transcription, including the mediator, TFIID, and Swi/Snf complexes [16,20]. These widespread interactions implicate Brd2 in targeting critical components of the transcriptional machinery to precisely modified regions of the eukaryotic genome.

While distinct interactions and expression patterns of the mammalian BET proteins have been described, little is known about the potential function of Brd2 in normal mammalian development. Disruption of the Brd2-related paralog, Brd4, in the mouse leads to early post-implantation lethality *in vivo* and an inability to maintain the inner cell mass *in vitro* [21]. Recently, a single bromodomain of the testis-specific Brdt has been shown to be required for male germ cell differentiation [22]. These studies suggest that although the basic structure of related BET family members is conserved, their expression patterns and functions in mammalian development are diverse. A number of studies in mammalian cells have implicated Brd2 function in the positive control of cell proliferation. Brd2 has been shown to bind several E2F cell cycle transcriptional activators and its exogenous expression was shown to help activate the cyclin A promoter [18,19]. Moreover, specific over-expression of *Brd2* in the lymphoid lineage was shown to result in B cell lymphoma and leukemia [23]. Several studies have documented the nuclear accumulation of Brd2 during diverse proliferation events in cultured cells and in neural and reproductive tissues *in vivo* [16,23,24]. In an embryonic development study of the mouse, expression of *Brd2* mRNA peaked between E8.5 and E12.5 and was prominently detected in the developing CNS [24]. In humans, mutations in the promoter of the *BRD2* gene have been linked to increased susceptibility to juvenile myoclonic epilepsy (JME), an adolescent-onset generalized epilepsy [25]. *BRD2* has also been genetically linked to photoparoxysmal response (PPR), a related seizure disorder in humans [26].

Given the current known biochemical functions of Brd2 and its potential role in neural development and disease, we disrupted the *Brd2* gene in the mouse to investigate its biological function during mammalian development. Here, we show that Brd2-deficient embryos deviate from normal developmental programs at embryonic day 9.0 (E9.0), when they exhibit delayed development, later growth retardation and fail to survive after E13.5. Strikingly, as neural development progresses, Brd2-null embryos consistently manifest neural tube closure defects that most commonly appear as exencephaly of the hindbrain. Moreover, deregulation of transcription at E9.0 may underlie the developmental defects observed in the Brd2-null embryos before they become apparent. Together, these data indicate essential roles for Brd2 in regulating chromatin structure and transcription during mammalian development.

Materials and Methods

ES cells and generation of Brd2-null mice

The ES cells RREO50, which carry a gene-trap construct in between the first and second coding exons of *Brd2* (BayGenomics), were grown on mitotically inactive feeder layers until 90% confluent and were dissociated by trypsinization before injection. E3.5 blastocysts were derived from C57BL/6-Tyr$^{c\text{-}Brd}$ female mice and injected with 12–20 ES cells. The injected blastocysts were implanted into the uteri of day 2.5 pseudo-pregnant females, with eight to ten embryos implanted per uterine horn. The resulting male chimeras were mated with C57BL/6-Tyr$^{c\text{-}Brd}$ females to obtain F1 progeny. The strain carrying the germ line transmitted allele (named *Brd2*^{Gt1RFr} and hereafter referred to as minus allele) was maintained on a mixed C57BL/6-129Ola background. Heterozygous animals were intercrossed to produce *Brd2*$^{+/+}$, *Brd2*$^{+/-}$ and *Brd2*$^{-/-}$ embryos. A second gene-trapped ES cell line from EUCOMM (OTTMUSG00000017279) was used to derive a second disrupted *Brd2* mouse line (named *Brd2*^{Gt2RFr} and hereafter referred to as the lacZ allele). All breeding and procedures were carried out according to institutional regulations at Brown University Animal Facility and NIH Guide for the Use and Care of Laboratory Animals.

PCR genotyping

To differentiate wild-type (+) from mutant (−) alleles of *Brd2*, a 551bp amplicon of the mutant allele was PCR-amplified using Brd2For5-GTTCCCTGAGGTCAAGATGCTG and βGalRev7-ACCCCTTCCTCCTACATAGTTGGC and subsequently sequenced to identify the junction between the endogenous sequence and the insertion cassette. This analysis uncovered that 417 bp at the 5′-end of the gene trap was lost when it incorporated into the genome. However, the splice acceptor essential for the function of this disruption vector was retained. To identify the wild-type allele, a pair of primers, Brd2For1-GCTGAGCGGCGGCGGTTCCC proximal to Brd2For5 and Brd2IntRev93-CGGAACGCCGCCCCCCAACC downstream of the insertion cassette junction, were used to generate an amplification product of 106 bp. When resolved on 2% agarose-TAE gels stained with ethidium bromide, these two PCR products allowed us to identify genomic DNA of all three genotypes. Genomic DNA was isolated from either adult mouse-tail biopsies or yolk sacs of developing embryos using the DNeasy Blood & Tissue Kit (Qiagen) according to manufacturer's instructions.

Embryo Dissection and RNA Preparation

Female mice of *Brd2* heterozygous intercrosses were checked every morning for the presence of a copulation plug. The day on which the copulation plug was observed was designated as E0.5. Dissections took place on subsequent days of development. Females were sacrificed and the uterine horns were excised and placed in sterile PBS. Decidual swellings corresponding to embryos were dissected individually, and yolk sacs retained for PCR genotyping. Resultant embryos were imaged using a Zeiss Discovery V8 stereomicroscope equipped with an Axiocam MRc camera and Axiovert software. Immediately after imaging, embryos were dounced in Trizol (Invitrogen) to preserve RNA quality, and RNA was isolated using manufacturer's protocols.

Microarray

Total RNA from nine E9.0 embryos (3 *Brd2*$^{+/+}$, 3 *Brd2*$^{+/-}$, 3 *Brd2*$^{-/-}$) was obtained as described above and further purified using micro RNeasy columns (Qiagen). RNA quality was checked using a Bioanalyzer, and concentration determined using a Nanodrop. 100 ng of each RNA sample were used in the Affymetrix Whole-transcript Sense Target Labeling Assay (Rev 3) followed by hybridization to a GeneChip® Mouse Gene 1.0 ST Array. Nine GeneChips were

used to provide biological triplicates of each genotype. The Affymetrix Expression Console (v 1.1) was used to normalize data and determine signal intensity (RMA-Sketch). Analysis was performed in Microsoft Excel. Transcripts with two-fold or greater changes in *Brd2*$^{-/-}$ embryos are reported in Supplemental Table 1.

Quantitative RT-PCR

RNA was isolated from E9.5 embryos collected from timed heterozygous matings as described earlier. RNA concentrations were determined by Nanodrop (Thermo Scientific), and 0.5 to 1 μg of total RNA was used to prepare 20 μl of cDNA using the iScript Select kit (BioRad). Real-time PCR reactions were performed in triplicate using 1 μl of cDNA template, SYBR green PCR master-mix (ABI) and gene-specific primers for *Brd2*, *Med26*, *Brachyury*, *NeuroD1*, *NeuroD4*, *Olig3*, *SlitRK6*, and *18S* rRNA (Invitrogen) in the ABI 7300 Real Time PCR System, according to manufacturers' protocols. Primer sequences can be found in Supplemental Table 2. Relative mRNA expression levels were determined using ΔCt values and were normalized to *18S* rRNA levels to correct for minor variations in starting RNA concentrations.

β-galactosidase, Phosphorylated-H3 and TUNEL staining

β-galactosidase staining of whole E13.0 embryos was performed using standard protocols. Freshly harvested embryos were fixed for 20 minutes at room temperature in 0.2% glutaraldehyde, washed three times in 0.1M phosphate buffer and incubated in 1 mg/ml X-gal (Invitrogen) overnight at room temperature. For immunostaining and TUNEL, freshly harvested embryos were fixed overnight at 4°C in 4% PFA, cryopreserved through serial incubation in 15% and 30% sucrose at 4°C, frozen in OCT blocks in liquid nitrogen and sectioned at 10 μm. For P-H3 antibody staining, slides were blocked for 1–2 hours in 10% goat serum and 10% BSA in PBT. Slides were then incubated at 1:100 dilution anti-P-H3 antibody (Cell Signaling, 9701S) in 10% goat serum, 10% BSA in PBT at 4°C overnight. The slides were washed three times in PBS at room temperature and incubated with a 1:100 dilution of goat anti-rabbit Alexa Fluor 594 (Molecular Probes, A11012) in 10% goat serum, 10% BSA in PBT for 2 hours at room temperature. For fluorescent analysis, the slides were washed three times in PBS, mounted with Vectashield plus DAPI (Vector Labs) and imaged on a Zeiss ImagerM1 fluorescence microscope using Axiovision software. For TUNEL staining, a Fluorescence In-Situ Cell Death Detection Kit (Roche) was utilized. Embryo sections were permeabilized for 6 minutes on ice in 0.1% Sodium Citrate, 0.1% Triton X-100 and rinsed twice in PBS. TUNEL substrate was mixed according to manufacturer's protocol (Roche). Slides were covered, placed in dark, humidified chambers and incubated at 37°C for one hour, rinsed three times in PBS, mounted with Vectashield plus DAPI (Vector Labs) and imaged on a Zeiss ImagerM1 fluorescence microscope.

Results

Gene trap-mediated disruptions of the mouse *Brd2* gene

To ascertain the functions of Brd2 in mouse development, a heterozygous embryonic stem (ES) cell line (RRE050) with a gene trap vector insertion in between the first two coding exons (Figure 1A) of the mouse *Brd2* gene was obtained from BayGenomics [27, 28]. The β-geo cassette of the gene-trap cassette contains a splice acceptor site which functions with the splice donor site of coding exon 1 of *Brd2* to produce a truncated *Brd2* transcript. This ES cell line was used to derive founder *Brd2* heterozygous (*Brd2*$^{+/-}$) mice. Initial genotyping of germ-line-transmitting founder *Brd2*$^{+/-}$ intercross progeny yielded viable wild type (*Brd*$^{+/+}$) and heterozygous (*Brd2*$^{+/-}$) progeny. However, intercrosses of heterozygous *Brd2* males and females failed to produce any *Brd2*$^{-/-}$ mice at weaning age (Figure 1B). Thus, this disruption of *Brd2* results in apparent embryonic or early postnatal lethality. Interestingly, the numbers of *Brd2*$^{+/-}$ progeny at weaning were lower than the expected Mendelian ratio of 2:1 (Figure

1B, p<0.0001). Therefore, having only a single functional copy of *Brd2* may have some deleterious effects on embryonic development, resulting in partially penetrant haploinsufficiency of heterozygous offspring.

Disruption of *Brd2* expression leads to embryonic lethality

The lack of viable $Brd2^{-/-}$ offspring suggested that Brd2 is required to complete embryogenesis. To characterize the role of Brd2 during embryogenesis, timed matings of $Brd2^{+/-}$ males and females were used to recover embryos across multiple developmental time points. PCR genotyping of yolk sac derived genomic DNA reliably detected embryos of all three *Brd2* genotypes in litters ranging from E8.5 to E13.5 from heterozygous intercrosses. To verify *Brd2* disruption by the insertion of the gene trap vector, quantitative RT-PCR (qPCR) was used to detect and quantify transcripts of *Brd2* and the β-galactosidase transgene in E9.5 in littermate embryos of all three *Brd2* genotypes. *Brd2* mRNA was undetectable in $Brd2^{-/-}$ embryos, while the relative *Brd2* mRNA level in $Brd2^{+/+}$ embryos was approximately two-fold higher than in $Brd2^{+/-}$ embryos (Figure 1C). Accordingly, $Brd2^{-/-}$ embryos were shown to have approximately two-fold higher expression of the β-galactosidase transgene relative to the $Brd2^{+/-}$ embryos. *Brd2* mRNA levels were normalized to *18S* rRNA levels to account for slight variation in total RNA yield from each individual embryo, and these experiments were repeated on multiple litters (data not shown). To assess the relative time of lethality, the progeny of multiple timed heterozygous intercrosses from E8.5 to E13.5 were recovered and genotyped. Of the 166 embryos recovered, 38 $Brd2^{-/-}$ embryos (23%) were identified between E8.5 and E11.5. In contrast, only 5 $Brd2^{-/-}$ embryos from a total of 59 recovered between E12 and E13 have been detected (8%; Table 1). At developmental stages E12 and later, uterine evidence of embryonic lethality was observed, which likely represents resorption of non-viable $Brd2^{-/-}$ embryos. These data indicate that only a fraction of the $Brd2^{-/-}$ embryos progress past E12, with a continuum of embryonic lethality occurring through several days (E8.5 to E11.5) during mid-gestation.

Developmental delay and neural tube closure defects of Brd2-null embryos

Phenotypic analysis of multiple embryonic litters derived from *Brd2* heterozygous intercrosses revealed fully penetrant severe growth retardation and defects in neural tube closure for $Brd2^{-/-}$ embryos compared to matched wild type littermates. Representative whole embryo images of wild type and $Brd2^{-/-}$ littermates from E9.0 to E13.5 are shown (Figure 2). Comparison of wild type and $Brd2^{-/-}$ embryos reveals a reduction in the overall size of the $Brd2^{-/-}$ embryos compared to matched wild type littermates. Severe growth retardation and developmental delay are most obvious at E9.0, when some $Brd2^{-/-}$ embryos are significantly smaller than their wild type counterparts and have not undergone axial rotation (Figure 2A and 2C). This lag in development was observed in 60% of Brd2-null embryos recovered at this early time point. Since most $Brd2^{-/-}$ embryos fail to develop past E12 (Table 1), it is likely that this severe developmental delay has lethal consequences for most embryos that fail to express *Brd2*. As development proceeds, all of the $Brd2^{-/-}$ embryos display cranial defects in neural tube closure (Figure 2E-P). Most $Brd2^{-/-}$ embryos do complete axial rotation, and the most common neurodevelopmental defect observed is exencephaly in the developing hindbrain region (Figure 3). The neural folds in the rhombencephalon are large, thickened, and splayed open to the outside of the embryo (Figure 2, M-P and Figure 3). Additionally, multiple $Brd2^{-/-}$ embryos display a curved caudal neural tube with frequent openings within the neural region (Figure 4). In contrast, other aspects of development such as limb, heart and somite development appear relatively intact in the older $Brd2^{-/-}$ embryos (Figure 2, M-P). The neural tube defects of the $Brd2^{-/-}$ embryos are fully penetrant, as a $Brd2^{-/-}$ embryo with proper neurulation (n=43) has not been detected; however, the defects are pleiotropic in nature. In addition, several heterozygous $Brd2^{+/-}$ embryos have been identified with similar neural tube defects, although variable in nature (Supplemental Figure 1). Taken together, these data

indicate that Brd2 function is necessary for proper neural tube closure during embryonic development and suggest that Brd2 may play an essential role in the regional specification of the developing rhombencephalon.

High expression of *Brd2* in the developing neural tube

To address the localization of Brd2 function during mouse embryonic development, the expression of a β-galactosidase reporter gene in a second targeted *Brd2* strain (Figure 1A), derived from an EUCOMM ES cell line, was used to examine the endogenous expression pattern of *Brd2* in developing embryos. $Brd2^{Gt2RFr}$ mice demonstrated embryonic β-galactosidase activity in genotypically $Brd2^{+/lacZ}$ versus matched wild type $Brd2^{+/+}$ control embryos. Much of the light blue β-galactosidase staining is readily detectable on the inside of the E13.0 embryos (Figure 5). Strikingly, β-galactosidase staining is most readily detected in the developing brain and spinal cord, precisely in the neural tube that fails to close properly in the $Brd2^{-/-}$ embryos. This neural-specific expression pattern is consistent with an RNA in situ pattern reported in a previous study of *Brd2* expression during mouse embryogenesis [24]. The heightened and localized expression of *Brd2*, together with the developmental defects in null mutants reported here, suggests a critical role in the development of the mouse CNS.

Proliferation and apoptosis in the developing Brd2-null neural folds

A number of diverse cellular processes are known to underlie proper neural tube closure in rodents and humans [29,30]. To begin to assess the cellular etiology of the neural tube defects associated with loss of Brd2, phosphorylated histone H3 (P-H3) and terminal deoxynucleotidyl transferase (TUNEL) staining were performed to detect proliferation and apoptosis, respectively. Cell proliferation in the thickened neural folds of the $Brd2^{-/-}$ embryo is evidenced by the nuclear staining of P-H3 on the ridges of the neural folds. The extent and localization of staining in the mutant, whose neural folds are spread apart, is similar, although not identical, to the wild type control, where the neural folds are bending towards each other (Figure 6A and B). Similarly, little difference in apoptosis is observed between the $Brd2^{+/+}$ and $Brd2^{-/-}$ embryos at this E11.5 time point (Fig. 6C and D). Together, these data indicate that there are no significant defects in cell proliferation and apoptosis in this $Brd2^{-/-}$ embryo at this time point; however, such cellular defects may arise in more severely affected embryos that are more difficult to assay or at different time points in development.

Gene expression profiling and quantitative RT-PCR reveal changes in neuronal gene expression

To assess global gene transcription in the $Brd2^{-/-}$ embryos, the expression profiles of $Brd2^{+/+}$, $Brd2^{+/-}$ and $Brd2^{-/-}$ embryos were compared at E9.5 by microarray analysis. The transcript levels of a number of genes were found to differ, with two-fold or greater enrichment found in 46 genes and two-fold or greater reduction seen in only 10 transcripts (Supplemental Table 1). A subset of the reduced transcripts in the $Brd2^{-/-}$ embryos encode several key neuronal regulators such as the neurogenic differentiation factors 1 and 4 (NeuroD1 and NeuroD4) and the oligodendrocyte transcription factor 3 (Olig3; Table 2). The ephrin receptor A3 (EphA3) and the integral membrane protein SLITRK6, which shares homology with the neurotrophin receptor family, were also found to be expressed at two to three fold lower levels in the $Brd2^{-/-}$ embryos by expression array (Table 2). The reduced expression of these genes was confirmed by quantitative RT-PCR of RNA extracted from additional $Brd2^{+/+}$ and $Brd2^{-/-}$ littermates, demonstrating a three fold reduction in NeuroD4 and SLITRK6 and a four fold reduction in NeuroD1 and Olig3 in the $Brd2^{-/-}$ embryos compared to $Brd2^{+/+}$ littermates (Figure 7A). To confirm that these expression changes were not due simply to differences in embryonic stage of development, additional quantitative RT-PCR was performed on $Brd2^{+/+}$ and $Brd2^{-/-}$ embryos with 37–39 somite pairs. Similar fold reductions between $Brd2^{+/+}$ and

Brd2$^{-/-}$ embryos were observed (Figure 7B). All gene expression levels were normalized to *18S* rRNA.

Discussion

Spina bifida is one of the most common birth defects worldwide, whereas juvenile myoclonic epilepsy (JME) is much less common; however, both may have links to *Brd2* deregulation. Spina bifida involves a posterior opening of the spinal cord. Brd2 may play an indirect or direct role in this neural development defect. The *curly tail* mouse has been an extensively studied model of spina bifida, and recent progress has implicated the reduced expression of the transcription factor encoding gene *Grainy-head-like-3 (Grhl3*) as being responsible for the opening of the posterior neuropore in this mutant [31–33]. As spina bifida is only partially penetrant in the *curly tail* strain, a number of *curly tail* modifier genes have been mapped in the mouse genome. Strikingly, one of these *curly tail* modifiers, *Mct1*, has been mapped to the HLA region of mouse chromosome 17, in close proximity to the *Brd2* gene [34]. Based on the neural tube defects of the Brd2-null embryos presented here, Brd2 and Grhl3 may collectively coordinate precise transcriptional events required for proper neural tube closure.

Mutations in the promoter of the human *BRD2* gene have been linked to increased susceptibility to juvenile myoclonic epilepsy (JME), an adolescent-onset generalized epilepsy [25]. In addition, *BRD2* has also been genetically linked to photoparoxysmal response (PPR), a related seizure disorder in humans [26]. It is worth noting that differences between null mutations in the mouse that elicit striking neurodevelopmental defects (this study) and more subtle regulatory mutations of the human *BRD2* promoter may have profoundly different consequences. The human mutations are predicted to alter the relative levels of *BRD2* expression in certain individuals and are not predicted to alter the full-length protein product [25]. This hypothesis posits a threshold model of *BRD2* expression and susceptibility to JME. Given the striking neural tube closure defects of the Brd2-null embryos, it is possible that subtle changes in *BRD2* expression may result in viable offspring with neurodevelopmental changes consistent with an increased susceptibility to seizures.

Given Brd2's diverse molecular interactions and its relevance to human neural developmental defects, a functional investigation of Brd2 in mammalian development was warranted. Using reverse genetics to establish a Brd2-null mouse line, we demonstrate that the disruption of the *Brd2* gene causes embryonic lethality. Brd2-null embryos deviate from normal developmental programs at embryonic day 9.0 (E9.0) where they exhibit developmental delay and generalized growth retardation. As development progresses, *Brd2*$^{-/-}$ embryos consistently manifest neural tube closure defects that most commonly appear as exencephaly of the hindbrain. This observation correlates with a high expression of *Brd2* in the developing CNS.

Consistent with the notion of Brd2's involvement in cell proliferation, we find an overall reduction in the growth potential of the *Brd2*$^{-/-}$ embryos compared to Brd2-containing embryos (Figure 2). However, in contrast to Brd4-null embryos which fail much earlier in development, Brd2-null embryos have traversed many cell division cycles to reach these time points [21]. Here, we observed similar neural epithelial proliferation in a *Brd2*$^{-/-}$ embryo compared to a matched wild type control and conclude that significant differences in proliferation are not apparent (Figure 6). However, we cannot rule out the possibility that subtle differences in proliferation may accumulate over time and detract from normal neuronal development. Defects in coordinated specification and proliferation of early neural tissue may be associated with the neural tube defects of the Brd2-null embryos [29,30,36]. Expression of *Brd2* mRNA peaks between E8.5 and E12.5, and is prominently detected in the developing CNS [24]. Thus, at approximately E8.5 when neuronal proliferation is initiated, Brd2 may be required to promote neurogenesis by regulating the gene expression networks required to drive

the expansion of newly born neuronal cell types [29]. The nuclear accumulation of Brd2 in multiple proliferating neuronal cell types is consistent with this notion [24]. Thus, the inability of neural folds to fuse might reflect the inability of the Brd2-null embryos to produce enough neuronal precursor cells during early CNS development. Alternatively, *Brd2*$^{-/-}$ embryos may be unable to execute the correct amount of neuronal apoptosis, as Brd2 has been previously shown to be induced during apoptosis in PC12 cells and in neurons; this function may be important also during early neurogenesis [37]. Thus, in the absence of Brd2, a subtle loss in the balance of proliferation and apoptosis may help establish an unmanageable expansion of neural precursor cells, which may result in an inability to correctly fuse the neural folds. Additionally, Brd2 function may be required outside of the developing neural ectoderm. This result would be similar to neural tube closure defects in *Twist* knockout mice in which head mesenchyme or neural crest derivatives are the root of neural tube closure defects [38,39]. Future studies will aim to distinguish these diverse, yet related, possibilities.

Other models which provide insight into *Brd2* function include the Drosophila *Brd2* ortholog, *fsh1,* and murine *Gcn5* mutants. A recent report indicates that *fsh1* mutants undergo homeosis of the head and tail region that may be similar in nature to the neuronal defects of the Brd2-null mouse embryos [40]. In this regard, genes that are known to be critical regulators of midbrain-hindbrain specification and regionalization during early neuronal development may also be targets of Brd2 function [41,42]. In a recent report by Bu *et al*., cranial neural tube closure defects, similar to that observed in the Brd2-null embryos, are described in homozygous *Gcn5* mutants, which contain a single point mutation in the catalytic core of the histone acetyltransferase (HAT) domain [43]. Disruption of a related HAT, *p300,* leads to similar hindbrain exencepahly as in the Brd2-null embryos [44]. In addition to HATs, disruptions of *de novo* DNA methyltransferases *Dnmt3b* and *Dnmt1o* in the mouse result in neural tube closure defects [45, 46]. As histone acetylation and DNA methylation are functionally linked in epigenetic regulation, it is possible that Brd2 might play a central role in stabilizing methylation marks on the developing mammalian genome required for proper neurulation. Thus, phenotypic variation in the Brd2-null mutants may reflect mosaic methylation patterns between individual embryos [45]. Future studies using conditional alleles of Brd2 will focus on the molecular mechanism of Brd2 in regulating the specification and regionalization of the developing mouse brain.

Supplementary Material

Refer to Web version on PubMed Central for supplementary material.

Acknowledgments

The authors would like to thank John Coleman, Gary Wessel, Angus Wilson and Mike Marr for critical input throughout these studies and for insightful comments on the manuscript. We thank John Wallingford, Mark Zervas, Stephen Brown and Nellwyn Hagan for input and expertise in assaying neuronal development. We thank Bill Skarnes, BayGenomics and EUCOMM for generously providing the gene-trapped ES cell lines used in our study. We thank Mandy Pereira and Erin Paul in the transgenic mouse core facility at Brown University for establishing the Brd2-deficient mouse lines. We thank Dr. Christoph Schorl and the Genomics and Proteomics Core Facility at Brown University for expertise with microarray analysis and qPCR. This research was supported in part by NIH/NCRR COBRE Award # P20RR015578 and Ellison Medical Foundation awards to R.N.F.

References

1. Jacobson RH, Ladurner AG, King DS, Tjian R. Structure and function of a human TAFII250 double bromodomain module. Science 2000;288:1422–1425. [PubMed: 10827952]
2. Ladurner AG, Inouye C, Jain R, Tjian R. Bromodomains mediate an acetyl-histone encoded antisilencing function at heterochromatin boundaries. Mol Cell 2003;11:365–376. [PubMed: 12620225]

3. Dhalluin C, Carlson JE, Zeng L, He C, Aggarwal AK, Zhou MM. Structure and ligand of a histone acetyltransferase bromodomain. Nature 1999;399:491–496. [PubMed: 10365964]
4. Kanno T, Kanno Y, Siegel RM, Jang MK, Lenardo MJ, Ozato K. Selective recognition of acetylated histones by bromodomain proteins visualized in living cells. Mol Cell 2004;13:33–43. [PubMed: 14731392]
5. Yang XJ. Lysine acetylation and the bromodomain: a new partnership for signaling. Bioessays 2004;26:1076–1087. [PubMed: 15382140]
6. Florence B, Faller DV. You bet-cha: a novel family of transcriptional regulators. Front Biosci 2001;6:D1008–1018. [PubMed: 11487468]
7. Jenuwein T, Allis CD. Translating the histone code. Science 2001;293:1074–1080. [PubMed: 11498575]
8. Matangkasombut O, Buratowski RM, Swilling NW, Buratowski S. Bromodomain factor 1 corresponds to a missing piece of yeast TFIID. Genes Dev 2000;14:951–962. [PubMed: 10783167]
9. Matangkasombut O, Buratowski S. Different sensitivities of bromodomain factors 1 and 2 to histone H4 acetylation. Mol Cell 2003;11:353–363. [PubMed: 12620224]
10. Chang YL, King B, Lin SC, Kennison JA, Huang DH. A double-bromodomain protein, FSH-S, activates the homeotic gene ultrabithorax through a critical promoter-proximal region. Mol Cell Biol 2007;27:5486–5498. [PubMed: 17526731]
11. Digan ME, Haynes SR, Mozer BA, Dawid IB, Forquignon F, Gans M. Genetic and molecular analysis of fs(1)h, a maternal effect homeotic gene in Drosophila. Dev Biol 1986;114:161–169. [PubMed: 3007240]
12. Huang DH, Dawid IB. The maternal-effect gene fsh is essential for the specification of the central region of the Drosophila embryo. New Biol 1990;2:163–170. [PubMed: 1982070]
13. Rhee K, Brunori M, Besset V, Trousdale R, Wolgemuth DJ. Expression and potential role of Fsrg1, a murine bromodomain-containing homologue of the Drosophila gene female sterile homeotic. J Cell Sci 1998;111(Pt 23):3541–3550. [PubMed: 9811568]
14. Shang E, Salazar G, Crowley TE, Wang X, Lopez RA, Wang X, Wolgemuth DJ. Identification of unique, differentiation stage-specific patterns of expression of the bromodomain-containing genes Brd2, Brd3, Brd4, and Brdt in the mouse testis. Gene Expr Patterns 2004;4:513–519. [PubMed: 15261828]
15. Trousdale RK, Wolgemuth DJ. Bromodomain containing 2 (Brd2) is expressed in distinct patterns during ovarian folliculogenesis independent of FSH or GDF9 action. Mol Reprod Dev 2004;68:261–268. [PubMed: 15112318]
16. Crowley TE, Kaine EM, Yoshida M, Nandi A, Wolgemuth DJ. Reproductive cycle regulation of nuclear import, euchromatic localization, and association with components of Pol II mediator of a mammalian double-bromodomain protein. Mol Endocrinol 2002;16:1727–1737. [PubMed: 12145330]
17. Denis GV, Green MR. A novel, mitogen-activated nuclear kinase is related to a Drosophila developmental regulator. Genes Dev 1996;10:261–271. [PubMed: 8595877]
18. Denis GV, Vaziri C, Guo N, Faller DV. RING3 kinase transactivates promoters of cell cycle regulatory genes through E2F. Cell Growth Differ 2000;11:417–424. [PubMed: 10965846]
19. Sinha A, Faller DV, Denis GV. Bromodomain analysis of Brd2-dependent transcriptional activation of cyclin A. Biochem J 2005;387:257–269. [PubMed: 15548137]
20. Denis GV, McComb ME, Faller DV, Sinha A, Romesser PB, Costello CE. Identification of transcription complexes that contain the double bromodomain protein Brd2 and chromatin remodeling machines. J Proteome Res 2006;5:502–511. [PubMed: 16512664]
21. Houzelstein D, Bullock SL, Lynch DE, Grigorieva EF, Wilson VA, Beddington RS. Growth and early postimplantation defects in mice deficient for the bromodomain-containing protein Brd4. Mol Cell Biol 2002;22:3794–3802. [PubMed: 11997514]
22. Shang E, Nickerson HD, Wen D, Wang X, Wolgemuth DJ. The first bromodomain of Brdt, a testis-specific member of the BET sub-family of double-bromodomain-containing proteins, is essential for male germ cell differentiation. Development 2007;134:3507–3515. [PubMed: 17728347]

23. Greenwald RJ, Tumang JR, Sinha A, Currier N, Cardiff RD, Rothstein TL, Faller DV, Denis GV. E mu-BRD2 transgenic mice develop B-cell lymphoma and leukemia. Blood 2004;103:1475–1484. [PubMed: 14563639]
24. Crowley T, Brunori M, Rhee K, Wang X, Wolgemuth DJ. Change in nuclear-cytoplasmic localization of a double-bromodomain protein during proliferation and differentiation of mouse spinal cord and dorsal root ganglia. Brain Res Dev Brain Res 2004;149:93–101.
25. Pal DK, Evgrafov OV, Tabares P, Zhang F, Durner M, Greenberg DA. BRD2 (RING3) is a probable major susceptibility gene for common juvenile myoclonic epilepsy. Am J Hum Genet 2003;73:261–270. [PubMed: 12830434]
26. Lorenz S, Taylor KP, Gehrmann A, Becker T, Muhle H, Gresch M, Tauer U, Sander T, Stephani U. Association of BRD2 polymorphisms with photoparoxysmal response. Neurosci Lett 2006;400:135–139. [PubMed: 16516380]
27. Skarnes WC, von Melchner H, Wurst W, Hicks G, Nord AS, Cox T, Young SG, Ruiz P, Soriano P, Tessier-Lavigne M, Conklin BR, Stanford WL, Rossant J. A public gene trap resource for mouse functional genomics. Nat Genet 2004;36:543–544. [PubMed: 15167922]
28. Stryke D, Kawamoto M, Huang CC, Johns SJ, King LA, Harper CA, Meng EC, Lee RE, Yee A, L'Italien L, Chuang PT, Young SG, Skarnes WC, Babbitt PC, Ferrin TE. BayGenomics: a resource of insertional mutations in mouse embryonic stem cells. Nucleic Acids Res 2003;31:278–281. [PubMed: 12520002]
29. Copp AJ, Greene ND, Murdoch JN. The genetic basis of mammalian neurulation. Nat Rev Genet 2003;4:784–793. [PubMed: 13679871]
30. Harris MJ, Juriloff DM. Mouse mutants with neural tube closure defects and their role in understanding human neural tube defects. Birth Defects Res A Clin Mol Teratol 2007;79:187–210. [PubMed: 17177317]
31. Gustavsson P, Greene ND, Lad D, Pauws E, de Castro SC, Stanier P, Copp AJ. Increased expression of Grainyhead-like-3 rescues spina bifida in a folate-resistant mouse model. Hum Mol Genet. 2007
32. van Straaten HW, Copp AJ. Curly tail: a 50-year history of the mouse spina bifida model. Anat Embryol (Berl) 2001;203:225–237. [PubMed: 11396850]
33. Ting SB, Wilanowski T, Auden A, Hall M, Voss AK, Thomas T, Parekh V, Cunningham JM, Jane SM. Inositol- and folate-resistant neural tube defects in mice lacking the epithelial-specific factor Grhl-3. Nat Med 2003;9:1513–1519. [PubMed: 14608380]
34. Letts VA, Schork NJ, Copp AJ, Bernfield M, Frankel WN. A curly-tail modifier locus, mct1, on mouse chromosome 17. Genomics 1995;29:719–724. [PubMed: 8575765]
35. Chesnutt C, Burrus LW, Brown AM, Niswander L. Coordinate regulation of neural tube patterning and proliferation by TGFbeta and WNT activity. Dev Biol 2004;274:334–347. [PubMed: 15385163]
36. Wang S, Dibenedetto AJ, Pittman RN. Genes induced in programmed cell death of neuronal PC12 cells and developing sympathetic neurons in vivo. Dev Biol 1997;188:322–336. [PubMed: 9268578]
37. Chen ZF, Behringer RR. twist is required in head mesenchyme for cranial neural tube morphogenesis. Genes Dev 1995;9:686–699. [PubMed: 7729687]
38. Soo K, O'Rourke MP, Khoo PL, Steiner KA, Wong N, Behringer RR, Tam PP. Twist function is required for the morphogenesis of the cephalic neural tube and the differentiation of the cranial neural crest cells in the mouse embryo. Dev Biol 2002;247:251–270. [PubMed: 12086465]
39. Florence BL, Faller DV. Drosophila female sterile (1) homeotic is a multifunctional transcriptional regulator that is modulated by Ras signaling. Dev Dyn 2008;237:554–564. [PubMed: 18264999]
40. Zervas M, Blaess S, Joyner AL. Classical embryological studies and modern genetic analysis of midbrain and cerebellum development. Curr Top Dev Biol 2005;69:101–138. [PubMed: 16243598]
41. Voiculescu O, Taillebourg E, Pujades C, Kress C, Buart S, Charnay P, Schneider-Maunoury S. Hindbrain patterning: Krox20 couples segmentation and specification of regional identity. Development 2001;128:4967–4978. [PubMed: 11748134]
42. Bu P, Evrard YA, Lozano G, Dent SY. Loss of Gcn5 acetyltransferase activity leads to neural tube closure defects and exencephaly in mouse embryos. Mol Cell Biol 2007;27:3405–3416. [PubMed: 17325035]

43. Yao TP, Oh SP, Fuchs M, Zhou ND, Ch'ng LE, Newsome D, Bronson RT, Li E, Livingston DM, Eckner R. Gene dosage-dependent embryonic development and proliferation defects in mice lacking the transcriptional integrator p300. Cell 1998;93:361–372. [PubMed: 9590171]

44. Toppings M, Castro C, Mills PH, Reinhart B, Schatten G, Ahrens ET, Chaillet JR, Trasler JM. Profound phenotypic variation among mice deficient in the maintenance of genomic imprints. Hum Reprod 2008;23:807–818. [PubMed: 18276606]

45. Okano M, Bell DW, Haber DA, Li E. DNA methyltransferases Dnmt3a and Dnmt3b are essential for de novo methylation and mammalian development. Cell 1999;99:247–257. [PubMed: 10555141]

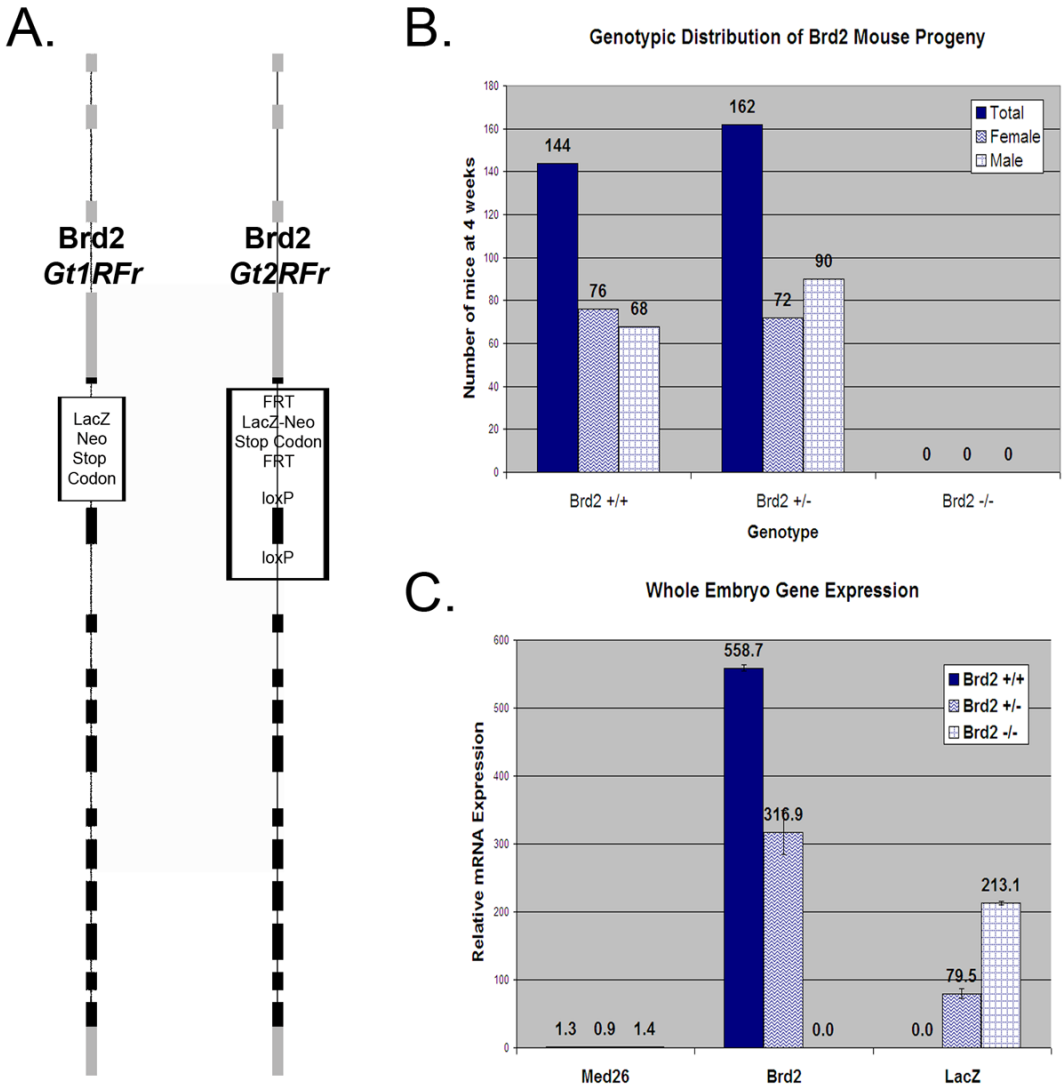

Figure 1.

Identification of Brd2-null embryos. (**A**) Schematic of genomic *Brd2* loci with insertions of two independent gene trap constructs between the first and second coding exons. (**B**) *Brd2* genotypic distribution of viable mice at four weeks of age born to *Brd2* heterozygous intercrosses. Total number of mice and sex-distribution of *Brd2* genotypes are shown with wild type ($Brd2^{+/+}$), *Brd2* heterozygote ($Brd2^{+/-}$) and null homozygous *Brd2* mutants ($Brd2^{-/-}$). (**C**) Quantitative RT-PCR analysis of mRNA derived from whole E9.5 embryos across the three *Brd2* genotypes. Relative levels of *Brd2* mRNA and mRNA from the LacZ transgene are graphed from a wild type embryo (+/+), a *Brd2* heterozygous embryo (+/−) and a homozygous *Brd2* mutant embryo (−/−) derived from the same litter. Relative mRNA expression levels were determined using ΔCt values and were normalized to *18S* rRNA levels to correct for minor variations in starting RNA concentrations. The absence of signal in the $Brd2^{-/-}$ embryo indicates that this embryo is devoid of wild type *Brd2* transcript and represents a Brd2-null embryo. *LacZ* expression was only detected in the *Brd2* heterozygous embryo (+/−) and the homozygous *Brd2* mutant embryo (−/−) and *Med26* expression was assayed as a control. Numbers at the top of each column are relative expression values for each gene set.

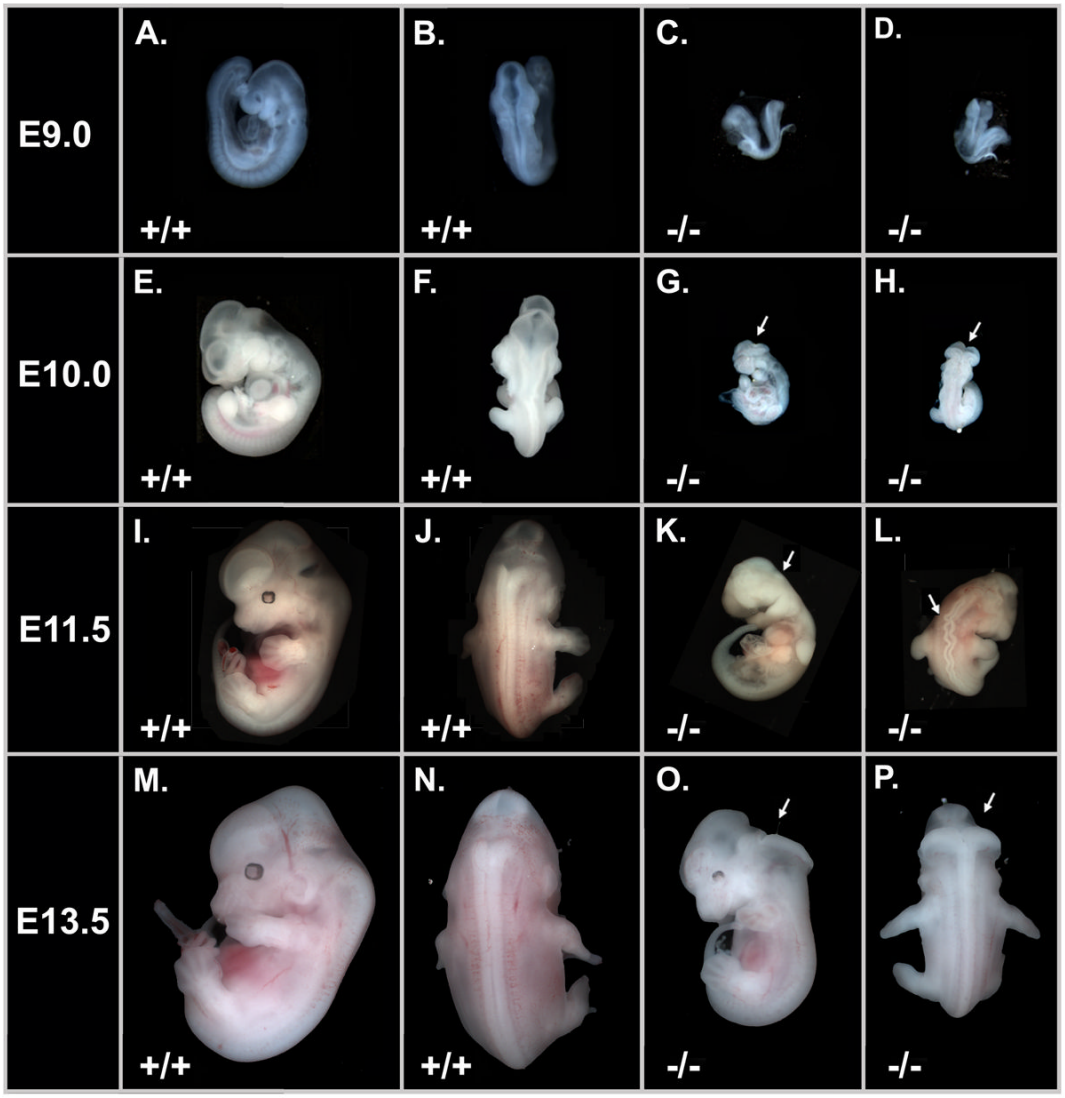

Figure 2.

Growth retardation and hindbrain exencephaly of Brd2-null embryos. Whole-mount analysis of matched wild type and Brd2-null embryos from E9.0–E13.5. Each embryo is represented by a side-by-side comparison of lateral and dorsal images. The genotypes of the embryos are as follows: (**A, B, E, F, I, J, M, N)** wild-type (+/+) embryos and (**C, D, G, H, K, L, O, P)** Brd2-null embryos. Note the marked decrease in overall size and the open neural tube (white arrows) at the level of the mesencephalon (**G, H**) and rhombencephalon (**K, L, O, P**) of the Brd2-null embryos. The four images at each time point are shown at identical magnification.

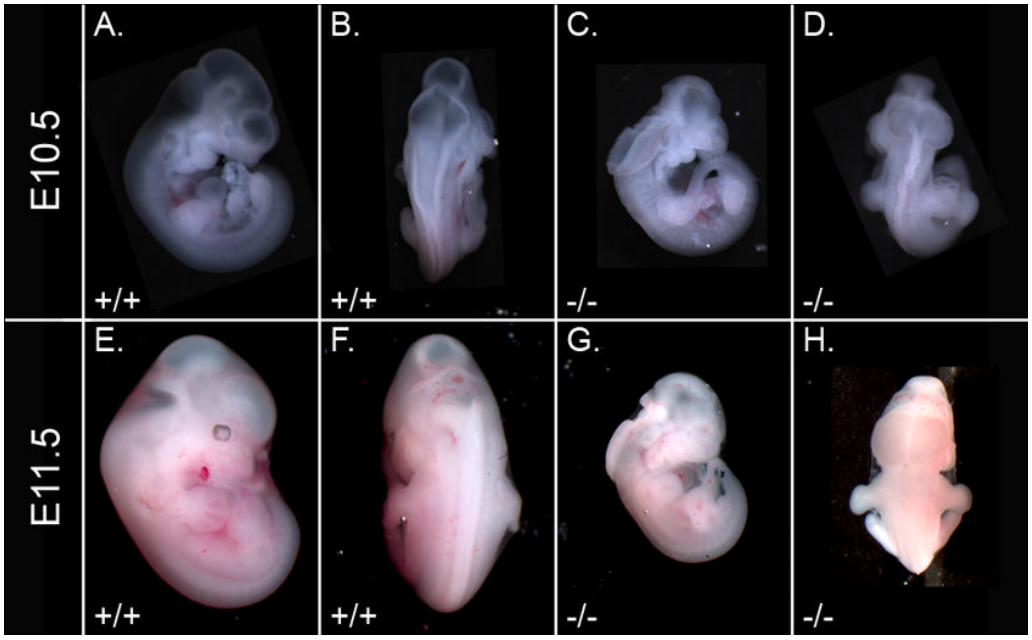

Figure 3.

Hindbrain exencephaly of *Brd2*$^{-/-}$ embryos at E10.5 and E11.5. Whole-mount analysis of littermate *Brd2*$^{+/+}$ and *Brd2*$^{-/-}$ embryos demonstrate the open hindbrain region and thickening of the edges of the open neural tube. Note the wavy, thickened neural tube in the *Brd2*$^{-/-}$ E10.5 embryo. The four images at each time point are shown at identical magnification to illustrate relative size differences.

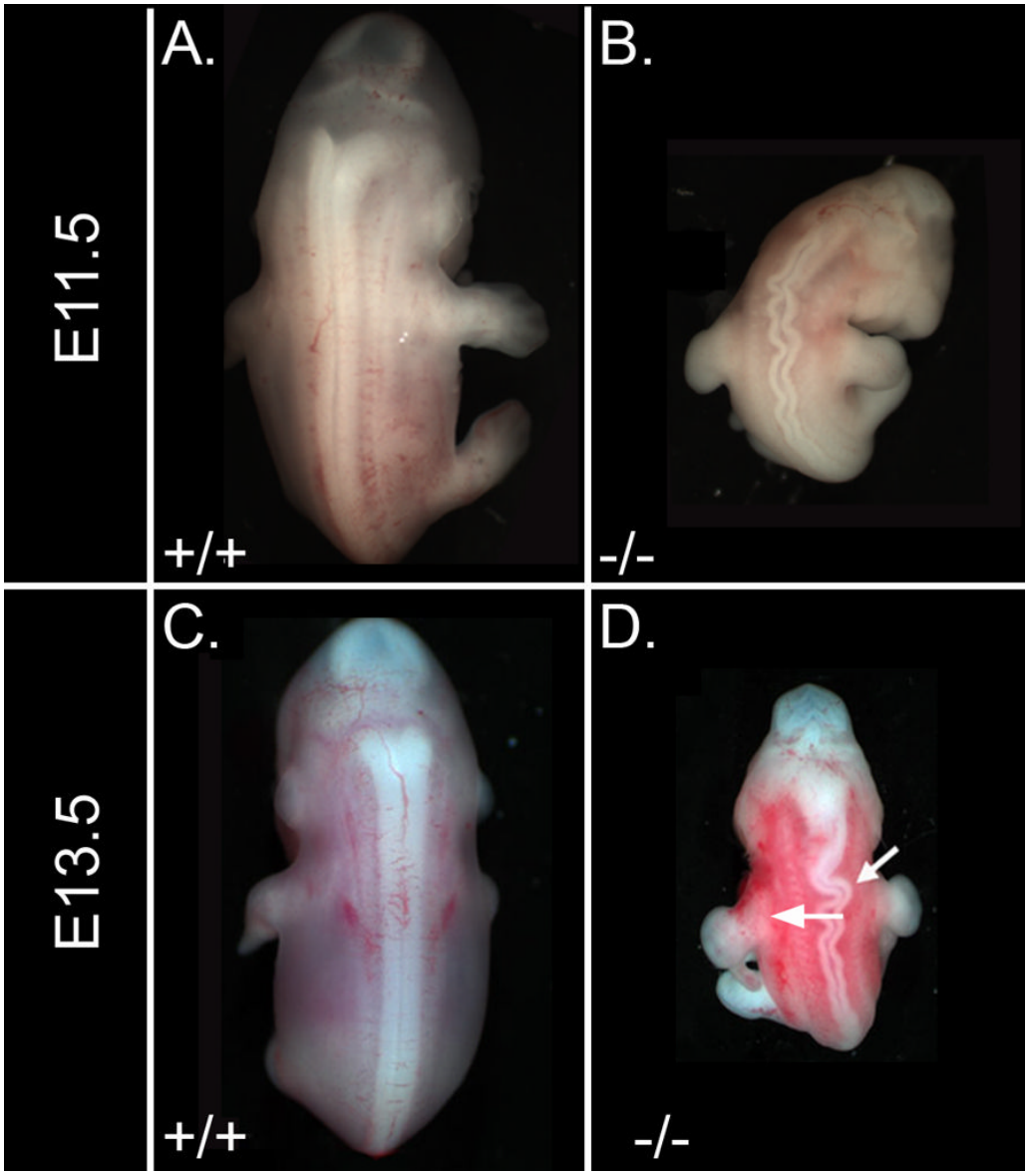

Figure 4.

The caudal neural tubes of *Brd2*$^{-/-}$ embryos display incomplete closure and frequent malformations. Whole-mount analysis of E13 *Brd2*$^{+/+}$ and *Brd2*$^{-/-}$ littermates from two separate heterozygous crosses illustrate the closure defects frequently found in Brd2-null embryos. Note the wavy, open neural tubes of the null embryos (white arrows) compared to wild-type littermates.

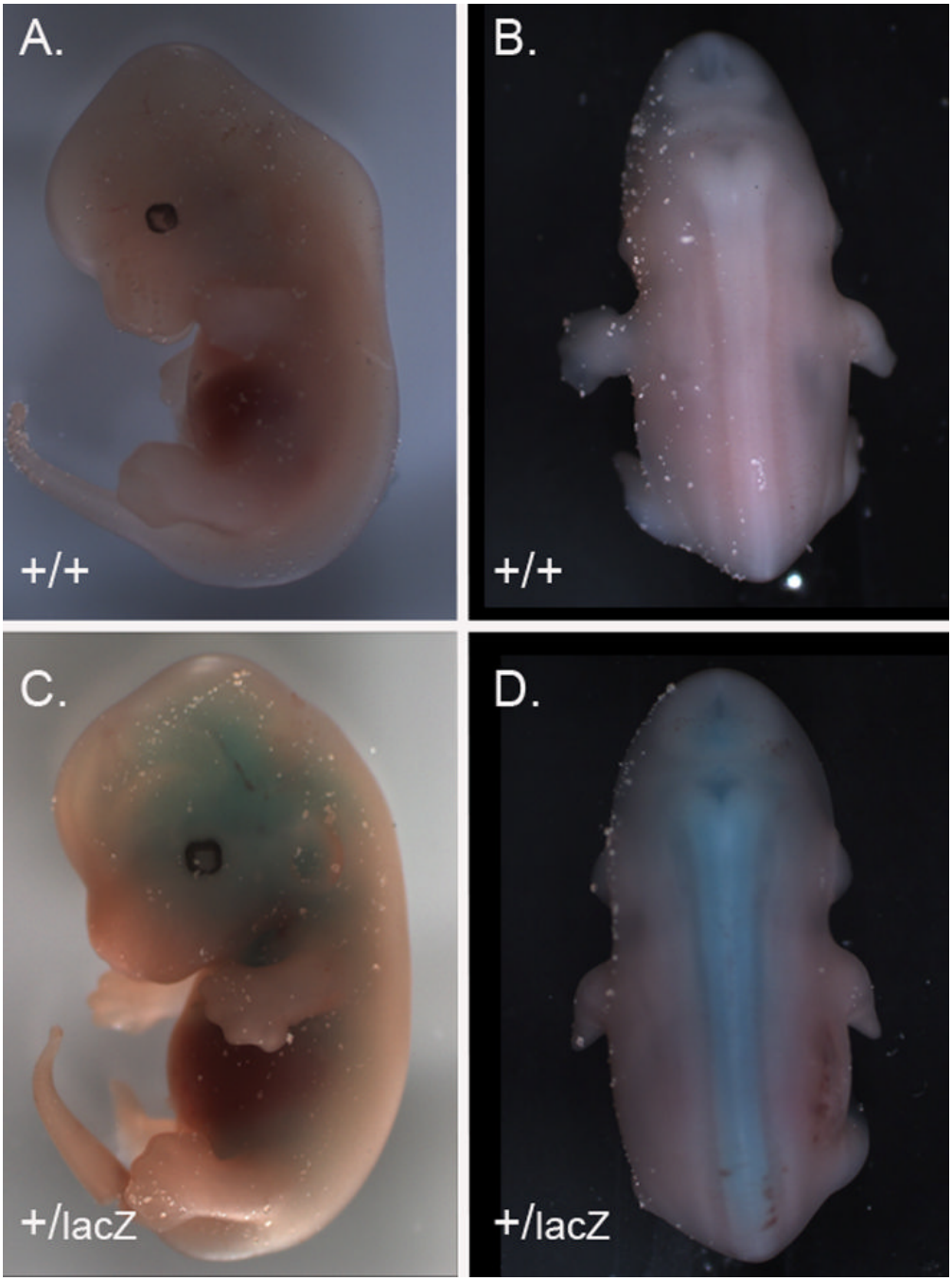

Figure 5.
Embryonic *Brd2* expression in the developing neural tube. A matched wild type (+/+, **A, B**) embryo and LacZ-containing *Brd2* heterozygous (+/LacZ, **C, D**) embryo from the same E13.0 litter is shown after β-galactosidase staining. Lateral (**A, C**) and dorsal (**B, D**) views are presented to highlight the expression of this *Brd2* reporter gene in the entire developing neural tube.

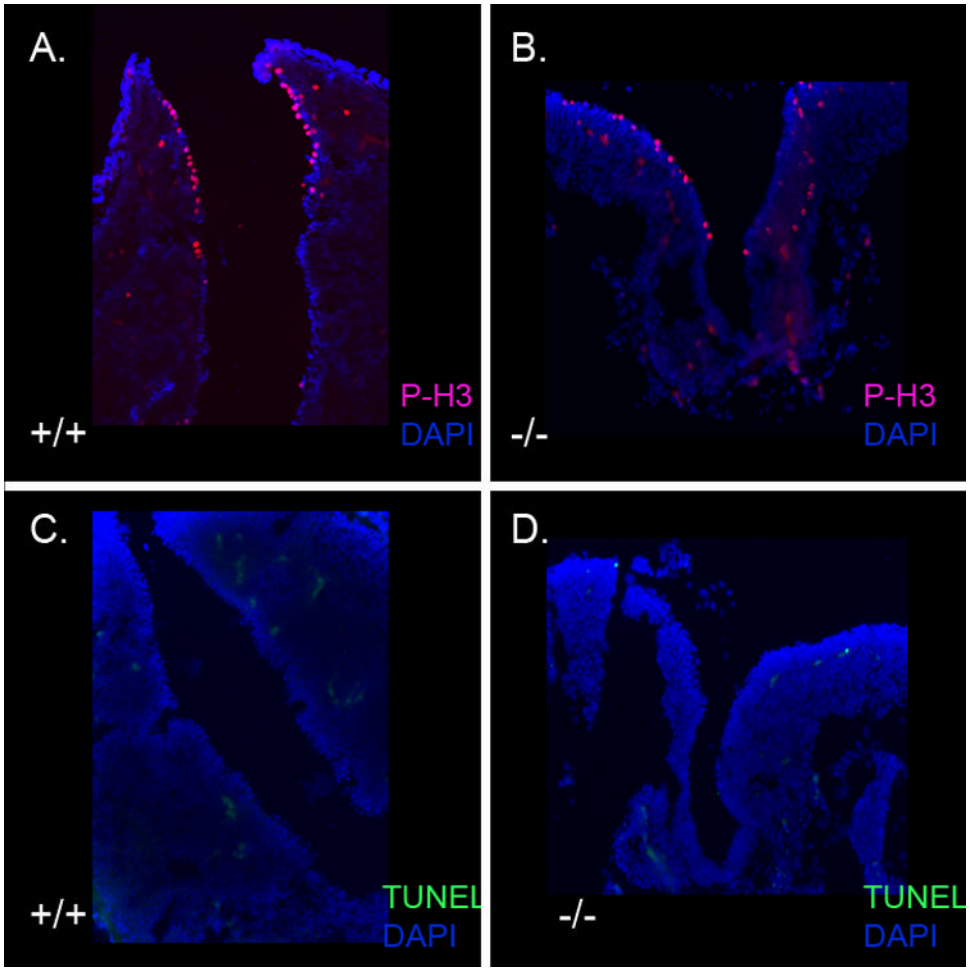

Figure 6.

Proliferation and apoptosis in the Brd2-null embryos. Sections from a matched wild type control (+/+, **A, C**) embryo and Brd2-null (−/−, **B, D**) embryo from the same E11.5 litter are shown after anti-phosphorylated histone H3 (**A**, **B**) and TUNEL staining (**C, D**). Phosphorylated histone H3 staining appears pink, TUNEL staining appears light green, and DAPI is shown in blue.

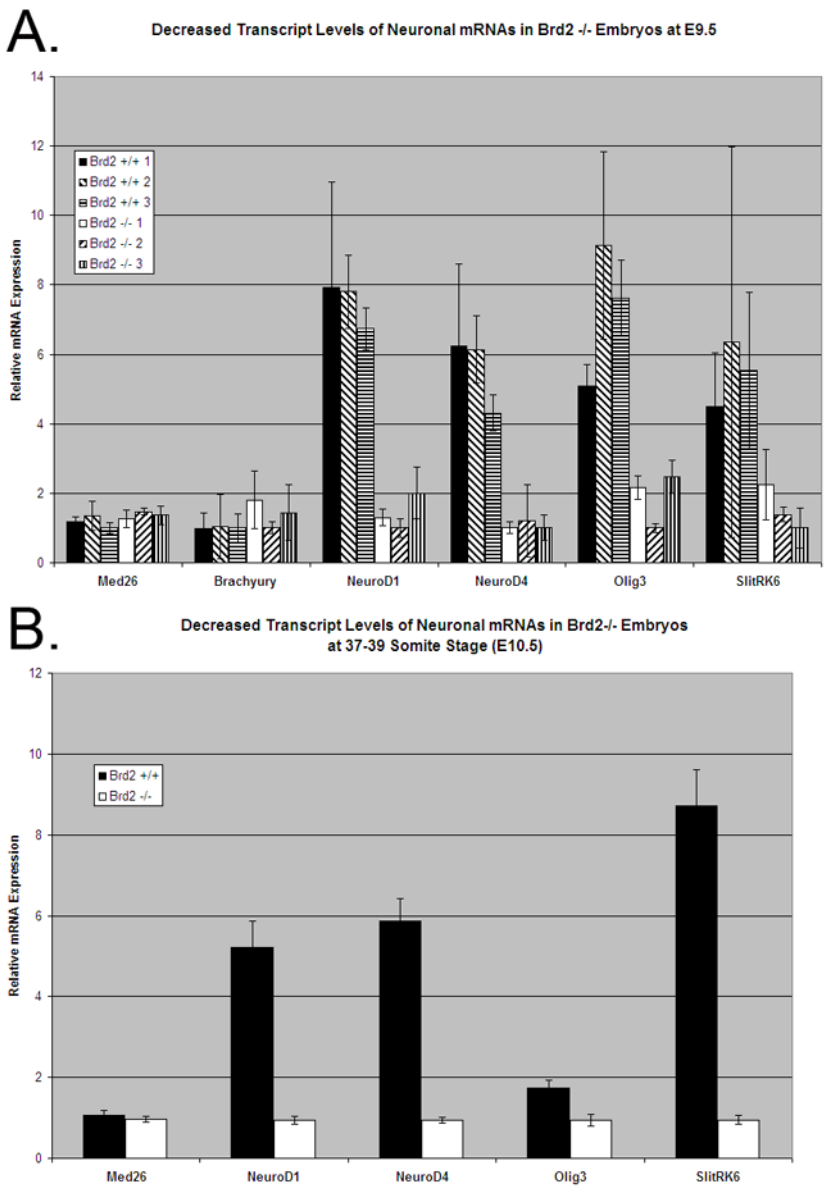

Figure 7.

Decreased transcript levels of neuronal mRNAs in *Brd2*$^{-/-}$ embryos. (**A)** Quantitative RT-PCR for mediator component *Med26* and mesodermal marker *Brachyury* (controls) show little relative difference between *Brd2*$^{+/+}$ and *Brd2*$^{-/-}$ embryos at E9.5, while mRNA levels of genes known to be involved in neuronal development *NeuroD1*, *NeuroD4*, *Olig3* and *SlitRK6* show a marked (3–4 fold) decrease in transcript level. (**B**) Expression of neuronal mRNAs in *Brd2*$^{+/+}$ and *Brd2*$^{-/-}$ embryos with 37–39 somites. Relative mRNA expression levels were determined using ΔCt values and were normalized to *18S* rRNA levels to correct for minor variations in starting RNA concentrations.

Table 1

Recovery of Brd2-null embryos during developmenta

Age	# Litters	*Brd2* +/+	*Brd2* +/−	*Brd2* −/−
E8–8.5	2	**4** (*3*)	**6** (*6*)	**2** (*3*)
E9–9.5	11	**29** *(23)*	**42***(46)*	**20** *(23)*
E10–10.5	4	**5** *(5)*	**10** *(11)*	**7** *(5)*
E11–11.5	4	**6** *(10)*	**26** *(21)*	**9** *(10)*
E12–12.5	3	**11** *(6)*	**11** *(12)*	**1** *(6)**
E13–13.5	3	**9** *(9)*	**23** *(18)*	**4** *(9)**
Total	27	**64** *(56)*	**118** *(114)*	**43** *(56)*

Numbers of recovered mouse embryos are shown in bold and expected numbers of embryos based on Mendelian ratios are shown in parentheses. Asterisks denote litters where reduced numbers of *Brd2*$^{-/-}$ embryos were recovered and increased numbers of resorbed embryos were detected.

Table 2

Genome-wide expression profiling reveals changes in global gene expression.

Gene	Description	Average Signal Intensity			Fold Change
		Brd2+/+	Brd2 +/−	Brd2 −/−	
Brd2	Bromodomain containing 2	1435	948	17	−81.7
Neurod1	Neurogenic differentiation 1	78	71	23	−3.33
Epha3	Eph receptor A3	105	91	32	−3.26
Slitrk6	SLIT and NTRK-like family, member 6	81	66	29	−2.74
Olig3	Oligodendrocyte transcription factor 3	141	162	59	−2.4
Neurod4	Neurogenic differentiation 4	96	112	40	−2.35

Microarray analysis revealed average expression values in biological triplicate embryos of each *Brd2* genotype. Each of these genes was expressed at statistically significant ($p<0.05$) reduced levels in the $Brd2^{-/-}$ and $Brd2^{+/-}$ embryos versus their age-matched wild type embryos. Fold change of these genes by microarray in the $Brd2^{-/-}$ embryos versus the wild type embryos is shown in the rightmost column.